Performance of a Double-multilayer Monochromator at Beamline 2-BM at the Advanced Photon Source

Y. S. Chu, C. Liu, D. C. Mancini, F. De Carlo, A. T. Macrander, B. Lai, D. Shu
Experimental Facilities Division, Argonne National Laboratory, IL, U.S.A.

Introduction

Multilayer optics, despite lacking a true crystalline structure, produce Bragg-like scattering because of their alternating periodic structure of high-Z (scatterer) and low-Z (spacer) elements, and they operate at a typical incident angle of one to a few degrees with a bandwidth about 100 times larger than crystal optics. Consequently, multilayer optics provide a significant flux increase for x-ray applications, such as imaging and fluorescence, where the narrow bandwidth of the crystal optics is not required.

Methods and Materials

A schematic diagram of the double-multilayer monochromator (DMM) is shown in Fig. 1, with the allowed linear and angular motions indicated. The design of the monochromator provides a fixed exit beam at 31 mm above the incident pink beam for the incident angular range of 1.35-1.90 [1, 2]. On the basis of this angular constraint, we have designed four multilayer structures needed for continuous operation of the DMM from 3.2 to 10.9 keV by using the first-order reflection (Table 1). The parameters for the two W/Si multilayers are optimized for the bandwidth, while the two W/C multilayers are designed to optimize the reflectivity in their operating energy ranges

The multilayer coatings were deposited by using a dc magnetron-sputtering deposition facility at the APS [3]. The two substrates were 100 × 146-mm monochromator-quality Si single crystals, polished to 1 Å rms roughness and 0.4 μmad average slope error. Four stripes were deposited separately in four successive depositions by using an appropriate stripe aperture. During the deposition, both substrates were mounted side by side along their length on a sample holder and scanned repeatedly over the two sputter guns that were turned on and off, synchronized to the motion of the sample holder. The velocity-controlled scanning helped remove the geometric effects of the sputtering and ensure a uniform multilayer structure along the longitudinal direction on both substrates. The uniformity of the multilayer structure along the transverse direction was ensured by using a shaped mask over the sputter guns. Under the deposition conditions used (1.5 to ~5-cm/s travel speed and sputter currents of 0.5, 0.6, and 0.7 A for W, C, and Si, respectively), 10 to ~17 h were required to complete the deposition of a stripe.

The multilayer coatings were characterized by using an x-ray reflectivity technique at the 2-BM bending magnet beamline of the APS by using a standard reflectivity experimental setup. The reflectivity measurements were carried out in two ways: by scanning the incident angle at a fixed incident beam energy of 10 keV and by scanning the incident beam energy at a fixed incident angle of 1.7°. The second method proved to be quite useful for probing the uniformity of the multilayer structure at various locations in the mirror with a small beam (50 × 50 μm), because the beam footprint remained constant during the entire measurement, which is not possible while scanning the incident angle.

Results

Table 1 summarizes the optical performance of all four stripes. The listed multilayer structures were obtained from fitting the reflectivity data measured at 10 keV, and the operating energy range of each stripe was determined from the fitted multilayer period based on an incident angular range of 1.35 to 1.9°. The reflectivity and bandwidth of the stripes in their operating energy ranges are based on selective measurements plus estimates from the simulation using the fit parameters. For all four stripes, the interlayer roughness/diffuseness obtained from fitting was 2 to ~3 Å. Measurements of the structural uniformity within a stripe as a function of position revealed a variation of about 1 to 2% in the bilayer thickness over the central region, while the structure of the two conjugate multilayer stripes exhibited better than 1% agreement in the distribution of the variation.

Discussion

At beamline 2-BM, there are two modes of operation for the DMM, as summarized in Fig. 2. In the normal operating mode, the pink beam reflected from a harmonic rejection mirror is incident on the DMM instead of on the Si(111) double-crystal monochromator (DCM). Consequently, the wide-bandpass beam from the DMM enters the end station at the same position as the monochromatic beam from the DCM; the DCM is effectively substituted by the DMM. The fixed exit beam requirement restricts the range of the incident beam angle to the first DMM mirror from 1.35 to 1.90°.

An extended mode of operation for the DMM is possible because of beamline 2-BM's capability of pink beam operation. In the pink beam configuration, the safety shutter and the beam collimator assembly, known as P6, drop down by 31 mm, allowing the pink beam from the harmonic rejection mirror to enter the end station. An 18-mm gap in P6 allows the DMM to be operated at incident angles from ~0.5 to 0.8°, giving access to a much wider energy range than originally intended. The practical upper energy limit is imposed by the broadening of the energy bandwidth near the critical angle of W and the decrease in the acceptance of the beam. In the extended energy range, the energy bandwidth, measured by a Ge energy-dispersive detector with a 0.2-keV energy resolution, ranged from 3 to 4%. In the normal operating mode, the DMM produces a flux 20-40 times greater than that of the Si(111) DCM as a result of the increased bandwidth. In the extended mode, however, the practical flux gain at energies above 13.5 keV is much greater because the current Si(111) DCM can reach these energies only by using a Si(333) reflection, which produces about 10 times lower flux.

Acknowledgments

Multilayer designing and data analysis were carried out by using the IMD software package [4]. Use of the APS was supported by the U.S. Department of Energy, Office of Science, Office of Basic Energy Sciences, under Contract No. W-31-109-ENG-38.

References

[1] Y. S. Chu, C. Liu, D. C. Mancini, F. De Carlo, A. T. Macrander, B. Lai, and D. Shu, Rev. Sci. Instrum. **73**, 1485 (2002).
[2] D. Shu, W. Yun, B. Lai, J. Barraza, and T. M. Kuzay, Rev. Sci. Instrum. **66**, 1786 (1995).
[3] C. Liu, J. Erdmann, J. Maj, and A. Macrander, J. Vac. Sci. Technol. **A17**, 2741 (1999); B. R. Thomas, D. Carter, and F. Rosenberger, J. Crystal Growth **187**, 499 (1998).
[4] D. L. Windt, Computers in physics **12**, 360-370 (1998). See http://cletus.phys.columbia.edu/windt/idl for downloading information and documentation.

Table 1. Summary of the performance of the DMM optics.

Stripe no.	Multilayer structure	Measured reflectivity at 10 keV (%)	Normal operating energy range (keV)	Reflectivity at operating energy range (%)	Bandwidth at operating energy range (%)
1	$[W(7.5)/Si(55.0)]_{35}$	78	3.2-4.6	~45	~5
2	$[W(9.7)/C(14.8)]_{100}$	65	8.0-10.9	~65	~1.5
3	$[W(14.2)/C(19.5)]_{50}$	82	6.1-8.1	~75	~5.5
4	$[W(6.8)/Si(36.0)]_{60}$	83	4.6-6.4	~65	~4

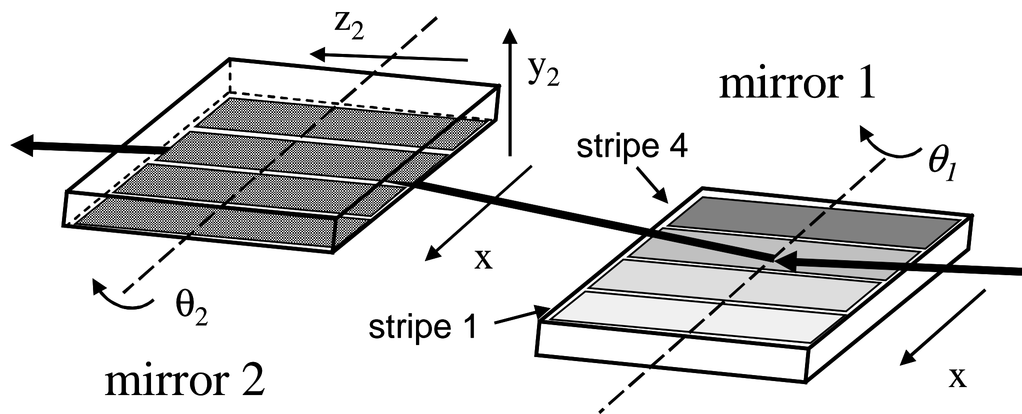

FIG. 1. (a) Schematic view of DMM with a fixed exit design. Each mirror is 100-mm wide and 146-mm long and contains four different stripes of coating in order to produce a continuous operating energy range from 3.2 to 10.9 keV. Stripes 1 through 4 are $[W(7.5)/Si(55.0)]_{35}$, $[W(9.7)/C(14.8)]_{100}$, $[W(14.2)/C(19.5)]_{50}$, and $[W(6.8)/Si(36.0)]_{60}$, respectively. The arrows indicate the independent (θ_1, θ_2, y_2, z_2) and coupled (x) motions allowed for the monochromator.

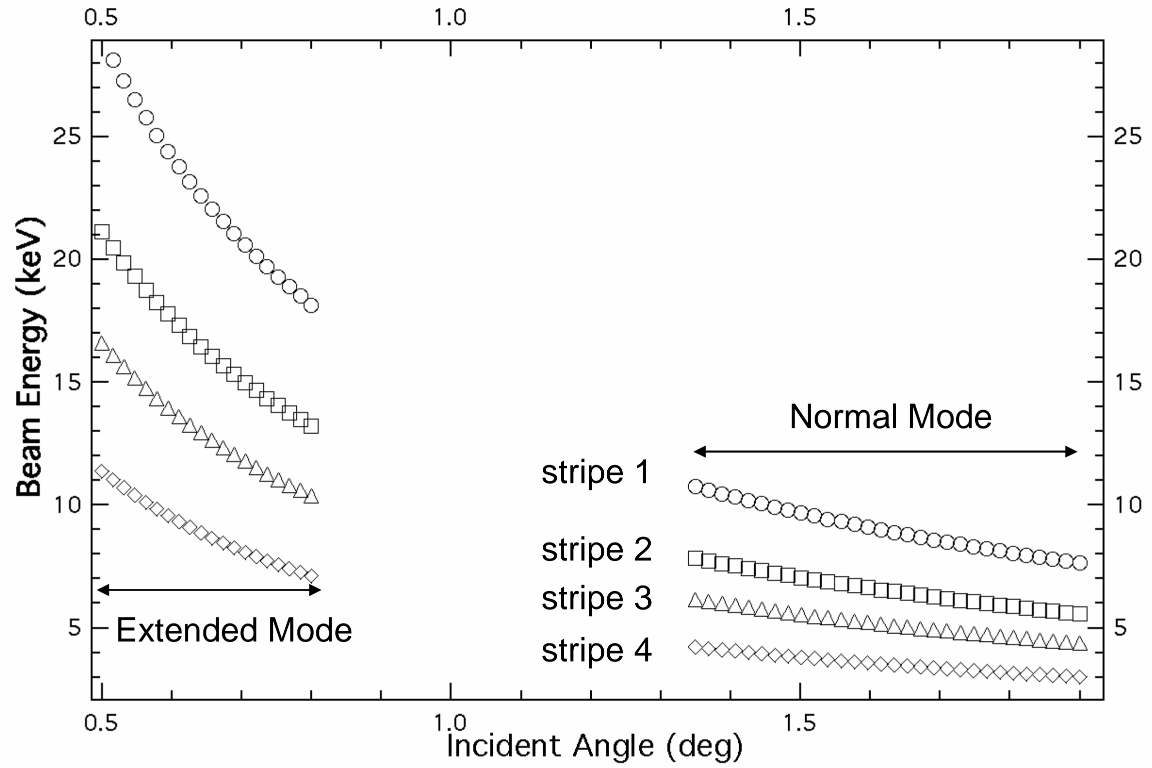

FIG. 2. Two operating modes of the DMM. In the normal operating mode, the four stripes cover the continuous energy range from 3.2 to 10.9 keV. The pink beam configuration of the beamline allows the extended operating mode up to 28 keV from stripe 2.